

# AN ITERATIVE SURE-LET DECONVOLUTION ALGORITHM BASED ON BM3D DENOISER

Feng Xue<sup>\*</sup>, Jizhou Li<sup>†</sup> and Thierry Blu<sup>‡</sup>

<sup>\*</sup>National Key Laboratory of Science and Technology on Test Physics and Numerical Mathematics, Beijing, 100076, China

<sup>†</sup>Howard Hughes Medical Institute, Stanford University, Stanford, CA 94305

<sup>‡</sup>Dept. of Electronic Engineering, The Chinese University of Hong Kong, Shatin, N.T., Hong Kong

## ABSTRACT

Recently, the plug-and-play priors (PPP) have been a popular technique for image reconstruction. Based on the basic iterative thresholding scheme, we in this paper propose a new iterative SURE-LET deconvolution algorithm with a plug-in BM3D denoiser. To optimize the deconvolution process, we linearly parametrize the thresholding function by using multiple BM3D denoisers as elementary functions. The key contributions of our approach are: (1) the linear combination of several BM3D denoisers with different (but fixed) parameters, which avoids the manual adjustment of a single non-linear parameter; (2) linear parametrization makes the minimization of Stein’s unbiased risk estimate (SURE) finally boil down to solving a linear system of equations, leading to a very fast and exact optimization during each iteration. In particular, the SURE of BM3D denoiser is approximately evaluated by finite-difference Monte-Carlo technique. Experiments show that the proposed algorithm, in average, achieves better deconvolution performance than other state-of-the-art methods, both numerically and visually.

**Index Terms**— Image deconvolution, Stein’s unbiased risk estimate (SURE), linear expansion of thresholds (LET), BM3D, finite-difference Monte-Carlo

## 1. INTRODUCTION

In this paper, we consider image deconvolution problem, i.e. to find a good estimate of original image  $\mathbf{x}_0 \in \mathbb{R}^N$  from the following image degradation model [1]:

$$\mathbf{y} = \mathbf{A}\mathbf{x}_0 + \mathbf{b} \quad (1)$$

where  $\mathbf{y} \in \mathbb{R}^N$  is the blurred noisy image,  $\mathbf{A} \in \mathbb{R}^{N \times N}$  denotes the convolution matrix constructed by point spread function,  $\mathbf{b}$  is often assumed as an additive white Gaussian noise with variance  $\sigma^2$ :  $\mathbf{b} \in \mathcal{N}(0, \sigma^2 \mathbf{I})$ .

There have been a large amount of literature on this topic. The regularization-based methods enforce a certain *explicit* prior (i.e. regularizer) on the original image  $\mathbf{x}_0$ , e.g. frame-based sparsity [2], total variation [3], FoE [4], MRF model

[5], and more complicated, possibly non-convex regularizers [6]. The related optimization algorithms typically include iterative shrinkage/thresholding (IST) [7] and alternating direction method of multipliers (ADMM) [8].

The key ingredient in both algorithms is the proximal operator associated with the regularizer, which is essentially an optimization problem corresponding to a simple denoising of intermediate solutions. The algorithms are able to decouple the handling of the convolution operator  $\mathbf{A}$  from that of the regularizer. To this end, the plug-and-play priors (PPP) have been proposed to replace the proximal mapping by the existing high-quality denoiser. For example, BM3D [9], WNNM [10], and NCSR [11] have been used to replace the proximal operator in IST, FISTA and ADMM for non-linear inverse scattering [12], tomographic reconstruction [13–15], and image superresolution [16]. Given more flexibility, the PPP scheme often yields better restoration quality than regularization-based methods, however, it fails to be interpreted as an optimization problem of a fixed cost function [12].

The SURE-LET methodology also provides an efficient and flexible framework for image denoising [17] and deconvolution [1, 18], which allows for the use of any existing solvers as the basis functions of the linear parametrization, and the optimal linear weights are automatically obtained by minimizing Stein’s unbiased risk estimate (SURE). Thanks to the quadratic nature of SURE, the optimization of the linear coefficients finally reduces to solving a low-order linear system of equations, that is very fast and exact [1, 17].

Combining the PPP idea and the SURE-LET framework, we in this work propose an iterative SURE-LET scheme, with the linear parametrization of thresholding function using several BM3D denoisers during each iterate. This leads to the fast and exact optimization of SURE, and achieves the state-of-the-art deconvolution performance.

## 2. SURE EVALUATION OF BM3D DENOISER

We begin with the SURE evaluation for the BM3D denoiser, which is necessary for the proposed SURE-LET algorithm.

Any estimated image  $\widehat{\mathbf{x}}$  can be expressed as a function of the observed image  $\mathbf{y}$  with some parameter  $\theta$ , i.e.  $\widehat{\mathbf{x}}_\theta = \mathbf{f}(\mathbf{y}; \theta)$ . In the context of pure denoising problem (i.e.  $\mathbf{A} = \mathbf{I}$  in (1)), the SURE of denoised image  $\widehat{\mathbf{x}}_\theta$  is given by [17, 19]:

$$\text{SURE} = \frac{1}{N} \|\widehat{\mathbf{x}}_\theta - \mathbf{y}\|_2^2 + \frac{2\sigma^2}{N} \text{Tr}(\mathbf{J}_y(\widehat{\mathbf{x}}_\theta)) - \sigma^2$$

which is an unbiased estimate of mean squared error (MSE), defined as  $\|\widehat{\mathbf{x}}_\theta - \mathbf{x}_0\|_2^2/N$ .

The BM3D is a complicated denoising procedure [9], thus, it is difficult to write the function  $\mathbf{f}$  in an explicit form, and exactly compute the Jacobian matrix  $\mathbf{J}_y(\widehat{\mathbf{x}}_\theta)$ . Instead, we simply treat the BM3D as a black box, and use finite-difference Monte-Carlo (FDMC) technique to approximate the trace term [19, 20]:

$$\text{Tr}(\mathbf{J}_y(\widehat{\mathbf{x}})) = \mathbb{E} \left\{ \mathbf{n}_0^\top \frac{\mathbf{f}(\mathbf{y} + \epsilon \mathbf{n}_0) - \mathbf{f}(\mathbf{y})}{\epsilon} \right\} \quad (2)$$

with a very small number  $\epsilon$ . Here,  $\mathbf{n}_0 \sim \mathcal{N}(\mathbf{0}, \mathbf{I})$  is a generated standard white Gaussian noise,  $\mathbf{f}(\mathbf{y} + \epsilon \mathbf{n}_0)$  denotes the BM3D denoised image with the input image being  $\mathbf{y} + \epsilon \mathbf{n}_0$ —a perturbed version of  $\mathbf{y}$ . In practice, we found that only one random realization of  $\mathbf{n}_0$  and  $\epsilon = 0.1\sigma$  could provide the sufficient accuracy for the trace computation.

Notice that the BM3D allows for an input parameter  $\theta$ , related to the noise standard deviation  $\sigma$  [9]. In general,  $\theta = \sigma$  yields the best denoising quality. To check the reliability of SURE (computed by FDMC) w.r.t. the actual MSE, we vary the BM3D parameter  $\theta$  by  $\theta = k \cdot \sigma$  with the factor  $k \in [0.1, 3.5]$ , and show the comparisons between SURE and MSE for each value of  $\theta$  in Fig.1. The closeness of the two curves demonstrates that the FDMC evaluation of SURE is accurate for the BM3D denoiser.

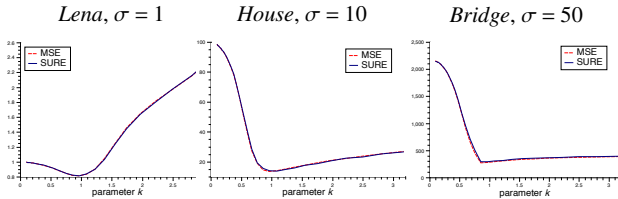


**Fig. 1.** MSE/SURE evaluations for BM3D denoising with various parameters  $k = \theta/\sigma$ .

### 3. THE BM3D-BASED ITERATIVE SURE-LET ALGORITHM

#### 3.1. The iterative thresholding scheme with BM3D denoiser

The general iterative thresholding algorithm takes the following form (assuming that  $\|\mathbf{A}\|_2 = 1$  for the normalized blur

kernel) [21]:

$$\begin{cases} \mathbf{z}^{(i)} &= \mathbf{y} - \mathbf{A}\mathbf{x}^{(i)} \\ \mathbf{u}^{(i)} &= \mathbf{x}^{(i)} + \mathbf{A}^\top \mathbf{z}^{(i)} \\ \mathbf{x}^{(i+1)} &= \mathcal{D}(\mathbf{u}^{(i)}; \theta^{(i)}) \end{cases} \quad (3)$$

where  $\mathbf{z}^{(i)}$  denotes the residual error of each step. The operation of  $\mathcal{D}(\cdot, \theta)$  performs denoising of input ‘noisy’ image  $\mathbf{u}^{(i)}$  for each iteration, with some parameter  $\theta^{(i)}$ . The simple soft/hard thresholding as  $\mathcal{D}$  (with  $\theta$  as a threshold) yields the famous IST/IHT algorithm [7]. Based on PPP scheme [12, 13], we propose to use BM3D denoiser as  $\mathcal{D}$  to solve image deconvolution. In addition, it is often suggested to choose the standard deviation of the residual error as the parameter value, i.e.  $\theta^{(i)} = \sigma^{(i)} = \sqrt{\|\mathbf{z}^{(i)}\|_2^2/N}$  [21].

#### 3.2. The proposed iterative SURE-LET scheme

However, we empirically found that the above choice of  $\theta^{(i)}$  is not optimal for the deconvolution problem. And, it is rather time consuming, if we use exhaustive search to find the optimal  $\theta^{(i)}$  by minimizing MSE of  $\|\mathbf{x}^{(i)} - \mathbf{x}_0\|_2^2/N$  for each step.

To speed up the optimization, we adopt the *linear expansion of thresholds* (LET) strategy [1, 17, 18, 22], i.e. represent the denoising function  $\mathcal{D}$  in (3) by a linear combination of a small number of BM3D denoisers with different, but fixed parameters  $\theta_k^{(i)}$ , i.e.

$$\mathbf{x}^{(i+1)} = \sum_{k=1}^K a_k^{(i)} \mathcal{D}(\mathbf{u}^{(i)}; \theta_k^{(i)}) = \mathbf{D}^{(i)} \mathbf{a}^{(i)} \quad (4)$$

where  $K$  is the number of linear coefficients  $a_k^{(i)}$  to be determined, and generally  $K \ll N$ .  $\mathbf{D}^{(i)} \mathbf{a}^{(i)}$  is a matrix notation, where  $\mathbf{D}^{(i)} = [\mathcal{D}(\mathbf{u}^{(i)}; \theta_1^{(i)}), \dots, \mathcal{D}(\mathbf{u}^{(i)}; \theta_K^{(i)})] \in \mathbb{R}^{N \times K}$ ,  $\mathbf{a}^{(i)} = [a_1^{(i)}, \dots, a_K^{(i)}]^\top \in \mathbb{R}^K$ . Now, the iterative deconvolution algorithm essentially amounts to finding the linear weights  $\mathbf{a}^{(i)}$ , such that the MSE

$$\text{MSE} = \frac{1}{N} \|\mathbf{x}^{(i+1)} - \mathbf{x}_0\|_2^2 \quad (5)$$

is minimized.

Since the actual MSE is not accessible in practice due to the unknown original image  $\mathbf{x}_0$ , we use the SURE as a practical substitute of MSE, given as [1, 19]<sup>1</sup>:

$$\text{SURE} = \|\mathbf{x}^{(i+1)}\|_2^2 - 2\mathbf{y}^\top \mathbf{A}^{-\top} \mathbf{x}^{(i+1)} + 2\sigma^2 \text{Tr}(\mathbf{A}^{-\top} \mathbf{J}_y(\mathbf{x}^{(i+1)})) \quad (6)$$

Substituting  $\mathbf{x}^{(i+1)}$  of (4) into the SURE (6), we obtain:

$$\begin{aligned} \text{SURE} &= \|\mathbf{D}^{(i)} \mathbf{a}^{(i)}\|_2^2 - 2\mathbf{y}^\top \mathbf{A}^{-\top} \mathbf{D}^{(i)} \mathbf{a}^{(i)} \\ &+ 2\sigma^2 \sum_{k=1}^K a_k^{(i)} \text{Tr}(\mathbf{A}^{-\top} \mathbf{J}_y(\mathcal{D}(\mathbf{u}^{(i)}; \theta_k^{(i)}))) \end{aligned} \quad (7)$$

<sup>1</sup>Here, we omit the factor  $1/N$  and the last constant term  $\|\mathbf{x}_0\|_2^2$  for brevity, since they are irrelevant to the optimization process.

Since the SURE is a quadratic function of  $\mathbf{a}^{(i)}$ , minimizing SURE w.r.t.  $\mathbf{a}^{(i)}$  boils down to solving a simple  $K$ -order linear system of equations:

$$(\mathbf{D}^{(i)})^T \mathbf{D}^{(i)} \mathbf{a}^{(i)} = (\mathbf{D}^{(i)})^T \mathbf{A}^{-1} \mathbf{y} - \sigma^2 \mathbf{c}^{(i)} \quad (8)$$

where  $\mathbf{c}^{(i)} = [c_1^{(i)}, \dots, c_K^{(i)}]^T \in \mathbb{R}^K$  with

$$c_k^{(i)} = \text{Tr}(\mathbf{A}^{-T} \mathbf{J}_y(\mathcal{D}(\mathbf{u}^{(i)}; \theta_k^{(i)})))$$

Thus, the solution to (8) automatically constitutes the best reconstruction performance for each step in terms of MSE/SURE.

The algorithm flowchart is summarized in Fig.2. The main computation of each iterate is to build and solve (8).

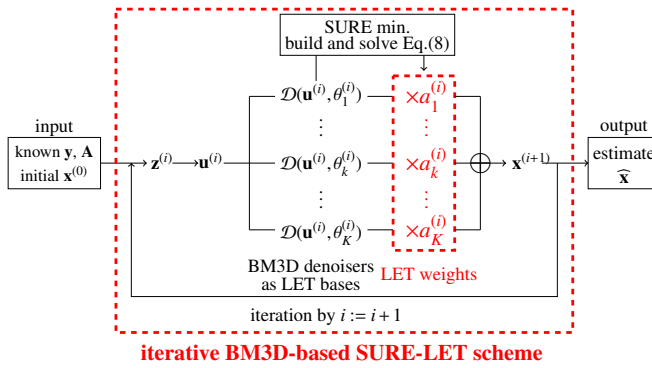


**Fig. 2.** The proposed iterative SURE-LET scheme based on BM3D denoiser.

It is also worth noting that the corresponding MSE minimization for each step leads to

$$(\mathbf{D}^{(i)})^T \mathbf{D}^{(i)} \mathbf{a}^{(i)} = (\mathbf{D}^{(i)})^T \mathbf{x}_0 \quad (9)$$

with the solution, namely *iterative MSE-LET*, serving as a counterpart to the iterative SURE-LET.

### 3.3. Implementation issues

Notice that the SURE requires to compute the inverse  $\mathbf{A}^{-1}$ , which may yield the numerical instability for the ill-conditioned  $\mathbf{A}$ . In practice, we use a regularized inverse  $\mathbf{A}_\beta^{-1}$  instead:

$$\mathbf{A}_\beta^{-1} = (\mathbf{A}^T \mathbf{A} + \beta \mathbf{I})^{-1} \mathbf{A}^T$$

with a parameter  $\beta$ . Experimentally, we found that  $\beta = 10^{-5} \sigma^2$  is a good choice for the accuracy.

Regarding the trace term of SURE, we apply FDMC in Section 2 to compute  $c_k^{(i)}$  for  $k = 1, 2, \dots, K$ :

$$\text{Tr}(\mathbf{A}_\beta^{-T} \mathbf{J}_y(\mathcal{D}(\mathbf{u}^{(i)}; \theta_k^{(i)}))) = \mathbb{E} \left\{ \left( \mathbf{A}_\beta^{-1} \mathbf{n}_0 \right)^T \frac{\mathcal{D}(\mathbf{u}_\epsilon^{(i)}) - \mathcal{D}(\mathbf{u}^{(i)})}{\epsilon} \right\}$$

where  $\mathbf{u}_\epsilon^{(i)}$  denotes the  $i$ -th update from the initial perturbed  $\mathbf{y} + \epsilon \mathbf{n}_0$ .

## 4. EXPERIMENTAL RESULTS AND DISCUSSIONS

### 4.1. Experimental setting

We consider 7 standard test images of size  $512 \times 512$ : *Lena*, *House*, *Bridge*, *California*, *Mandrill*, *Couple* and *Mixture*<sup>2</sup>. They are blurred by 4 typical kernels: (1) rational filter:  $h(i, j) = (1 + i^2 + j^2)^{-1}$  for  $i, j = -7, \dots, 0, \dots, 7$ ; (2) separable filter:  $[1 \ 4 \ 6 \ 4 \ 1]/16$  along both vertical and horizontal directions; (3)  $5 \times 5$  uniform blur; (4)  $9 \times 9$  uniform blur; and then contaminated by Gaussian noise with  $\sigma = 1, 5, 10, 30, 50, 100$ , respectively [1, 22, 24].

For our algorithm, we use  $K = 3$  BM3D denoisers with  $\theta_1^{(i)} = 0.1\sigma^{(i)}$ ,  $\theta_2^{(i)} = \sigma^{(i)}$  and  $\theta_3^{(i)} = 10\sigma^{(i)}$  for all test cases. We compare with recent high-quality deconvolvers, including SURE-LET deconv [1], BM3D-DEB [23], BM3D-IDD [24], NCSR [11], EPLL [25] and a learning-based method—MLP [26]<sup>3</sup>. The deconvolution performance is measured by the peak signal-to-noise ratio (PSNR), defined as (in dB) [1, 22, 24]:

$$\text{PSNR} = 10 \times \log_{10} \left( \frac{255^2}{\|\hat{\mathbf{x}} - \mathbf{x}_0\|^2 / N} \right)$$

### 4.2. Experimental results

First, we show the variations of PSNR by SURE/MSE-LET during the iterations in Fig.3, which demonstrates that the SURE-LET estimate is very close to that by MSE-LET.

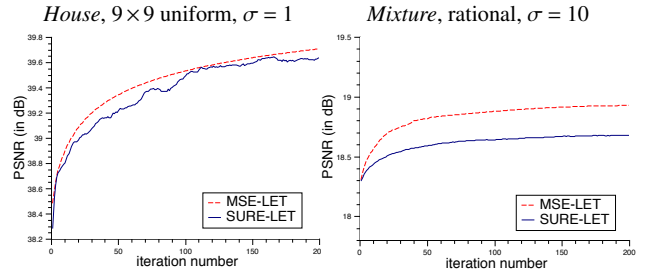


**Fig. 3.** Variations of PSNR during iterative SURE/MSE-LET process.

Due to the page limitation, Table 1 reports only the average PSNR results (in dB) of all the 7 images, under various blurs and noise levels. ‘ISL-BM3D’ and ‘IML-BM3D’ stand for our proposed BM3D-based iterative SURE/MSE-LET algorithms, where the results of *oracle MSE-LET* are shown in italics. The best PSNR results within 0.1dB margin are highlighted by boldface. Figs.4–5 show the visual comparisons between various methods.

<sup>2</sup>All the standard test images can be downloaded in [http://www.imageprocessingplace.com/root\\_files\\_v3/image\\_databases.htm](http://www.imageprocessingplace.com/root_files_v3/image_databases.htm).

<sup>3</sup>Note that the codes of NCSR [11] and MLP [26] do not contain the implementation of deconvolution with rational and separable filters. Thus, we cannot report the results in Table 1.

**Table 1.** PSNR comparison of some state-of-the-art deconvolution methods (in dB)

$\sigma$	1	5	10	30	50	100	1	5	10	30	50	100
blur type	rational filter						separable filter					
SURE-LET deconv [1]	32.10	26.84	25.17	22.94	22.02	<b>20.73</b>	32.17	28.96	27.36	24.62	23.29	<b>21.57</b>
BM3D-DEB [23]	32.08	26.94	25.12	22.61	21.60	19.97	32.16	29.20	27.54	24.65	23.24	20.83
BM3D-IDD [24]	31.95	27.29	25.27	22.76	21.65	20.07	32.50	29.64	28.00	24.87	23.30	21.07
EPLL [25]	29.35	25.84	24.23	22.13	21.37	17.45	30.10	28.45	27.05	24.28	23.05	17.88
ISL-BM3D	<b>32.74</b>	<b>27.63</b>	<b>25.84</b>	<b>23.24</b>	<b>22.26</b>	<b>20.81</b>	<b>33.22</b>	<b>29.91</b>	<b>28.20</b>	<b>25.09</b>	<b>23.55</b>	<b>21.60</b>
<i>IML-BM3D</i>	<i>32.91</i>	<i>27.76</i>	<i>25.91</i>	<i>23.27</i>	<i>22.27</i>	<i>20.82</i>	<i>33.30</i>	<i>29.96</i>	<i>28.26</i>	<i>25.13</i>	<i>23.57</i>	<i>21.60</i>
blur type	$5 \times 5$ uniform						$9 \times 9$ uniform					
SURE-LET deconv [1]	31.21	27.47	25.91	23.74	22.71	<b>21.32</b>	28.00	24.96	23.84	22.38	21.71	20.65
BM3D-DEB [23]	31.27	27.61	26.08	23.75	22.63	20.59	28.10	25.05	23.86	22.14	21.43	19.98
BM3D-IDD [24]	31.69	28.04	26.32	23.80	22.57	20.64	<b>28.78</b>	25.46	24.22	22.45	21.61	20.20
NCSR [11]	28.21	27.92	26.02	20.36	—	—	28.11	25.31	23.98	19.55	—	—
EPLL [25]	29.09	26.26	25.06	23.34	22.39	17.97	25.99	23.75	22.95	21.86	21.18	17.54
MLP [26]	25.99	25.58	25.19	24.03	22.84	20.88	25.74	24.92	24.13	22.48	21.63	20.36
ISL-BM3D	<b>32.08</b>	<b>28.23</b>	<b>26.61</b>	<b>24.16</b>	<b>22.99</b>	<b>21.33</b>	28.56	<b>25.70</b>	<b>24.52</b>	<b>22.79</b>	<b>21.99</b>	<b>20.77</b>
<i>IML-BM3D</i>	<i>32.24</i>	<i>28.31</i>	<i>26.70</i>	<i>24.24</i>	<i>23.01</i>	<i>21.34</i>	28.75	25.78	24.58	22.84	22.03	20.80



**Fig. 4.** Visual restoration quality (*Couple*,  $9 \times 9$  uniform,  $\sigma = 30$ ).

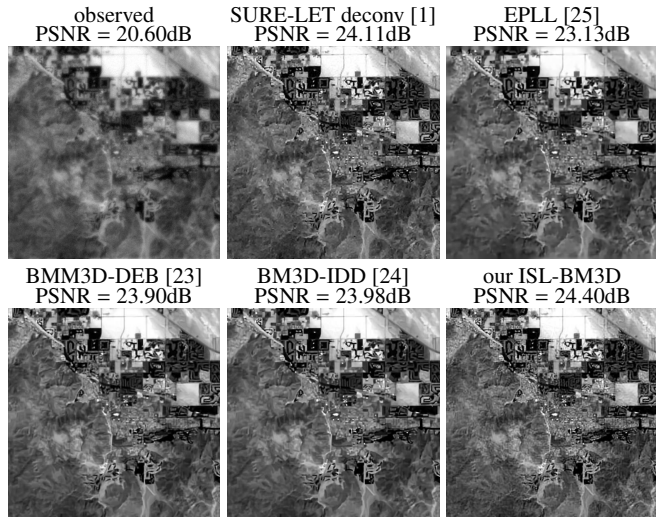


**Fig. 5.** Visual restoration quality (*California*, rational,  $\sigma = 5$ ).

We can see that compared to other state-of-the-art, the proposed ISL-BM3D achieves the best performance, and similar results with *IML-BM3D*. Recognizing that the BM3D denoiser is a key ingredient, we would also like to emphasize the advantage of the proposed iterative SURE-LET framework. From Table 1, we can see that the proposed algorithm outperforms BM3D-DEB and BM3D-IDD by, in average, 0.8dB and 0.5dB, which is a substantial improvement brought by the iterative SURE-LET optimization scheme.

## 5. CONCLUSIONS

In this paper, we presented a new iterative SURE-LET scheme for image deconvolution. Incorporating BM3D denoiser as the basis functions, this algorithm achieves the most

state-of-the-art performance. Notably, the proposed method provides a fast optimization framework of SURE-LET, and a flexible way by PPP for image deconvolution. In this paper, we use only 3 basis functions to demonstrate the effectiveness. One can expect better results, if incorporating more high-quality denoisers as the LET bases.

Future works may include the convergence analysis, faster algorithm/implementation and the better plug-in basis functions of SURE-LET.

## 6. ACKNOWLEDGMENTS

This work was supported by a grant CUHK14210617 from the Hong Kong research grant council.

## 7. REFERENCES

- [1] F. Xue, F. Luisier, and T. Blu, "Multi-Wiener SURE-LET deconvolution," *IEEE Trans. on Image Process.*, vol. 22, no. 5, pp. 1954–1968, 2013.
- [2] Stéphane Mallat, *A Wavelet Tour of Signal Processing: The Sparse Way*, 3rd edition, Academic Press, 2008.
- [3] L. I. Rudin, S. Osher, and E. Fatemi, "Nonlinear total variation based noise removal algorithms," *Physica D*, vol. 60, pp. 259–268, 1992.
- [4] S. Roth and M.J. Black, "Fields of Experts," *Int. J. Comput. Vis.*, vol. 82, no. 2, pp. 205–229, 2009.
- [5] S.C. Zhu and D. Mumford, "Prior learning and Gibbs reaction-diffusion," *IEEE Transactions on Pattern Analysis and Machine Intelligence*, vol. 19, no. 11, pp. 1236–1250, 1997.
- [6] P. Charbonnier, L. Blanc-Feraud, G. Aubert, and M. Barlaud, "Deterministic edge-preserving regularization in computed imaging," *IEEE Transactions on Image Processing*, vol. 6, no. 2, pp. 298–311, 1997.
- [7] Amir Beck and Marc Teboulle, "A fast iterative shrinkage-thresholding algorithm for linear inverse problems," *SIAM Journal on Imaging Sciences*, vol. 2, no. 1, pp. 183–202, 2009.
- [8] S. Boyd, N. Parikh, E. Chu, B. Peleato, and J. Eckstein, "Distributed optimization and statistical learning via the alternating direction method of multipliers," *Foundations and Trends in Machine Learning*, vol. 3, no. 1, pp. 1–122, 2011.
- [9] K. Dabov, A. Foi, V. Katkovnik, and K. Egiazarian, "Image denoising by sparse 3-D transform-domain collaborative filtering," *IEEE Trans. Image Process.*, vol. 16, no. 8, pp. 2080–2095, 2007.
- [10] Shuhang Gu, Lei Zhang, Wangmeng Zuo, and Xiangchu Feng, "Weighted nuclear norm minimization with application to image denoising," *Proc. IEEE Int. Conf. Comput. Vision and Pattern Recognition*, pp. 2862–2869, 2014.
- [11] Weisheng Dong, Lei Zhang, Guangming Shi, and Xin Li, "Nonlocally centralized sparse representation for image restoration," *IEEE Trans. Image Process.*, vol. 22, no. 4, pp. 1620–1630, 2013.
- [12] Ulugbek S. Kamilov, Hassan Mansour, and Brendt Wohlberg, "A plug-and-play priors approach for solving nonlinear imaging inverse problems," *IEEE Signal Processing Letters*, vol. 24, no. 12, pp. 1872–1876, 2017.
- [13] Suhas Sreehari, S. V. Venkatakrishnan, Brendt Wohlberg, Gregory T. Buzzard, Lawrence F. Drummy, Jeffrey P. Simmons, and Charles A. Bouman, "Plug-and-play priors for bright field electron tomography and sparse interpolation," *IEEE Transactions on Computational Imaging*, vol. 2, no. 4, pp. 408–423, 2016.
- [14] S.H. Chan, X. Wang, and O.A. Elgandy, "Plug-and-play admm for image restoration: Fixed-point convergence and applications," *IEEE Transactions on Computational Imaging*, vol. 3, no. 1, pp. 84–98, 2016.
- [15] Singanallur V. Venkatakrishnan, Charles A. Bouman, and Brendt Wohlberg, "Plug-and-play priors for model based reconstruction," *Proc. IEEE Global Conference on Signal and Information Processing*, pp. 945–948, 2013.
- [16] A. Brifman, Y. Romano, and M. Elad, "Turning a denoiser into a super-resolver using plug and play priors," *Proc. of IEEE International Conference on Image Processing*, pp. 1404–1408, 2016.
- [17] T. Blu and F. Luisier, "The SURE-LET approach to image denoising," *IEEE Transactions on Image Processing*, vol. 16, no. 11, pp. 2778–2786, 2007.
- [18] J. Li, F. Luisier, and T. Blu, "PURE-LET image deconvolution," *IEEE Trans. on Image Process.*, vol. 27, no. 1, pp. 92–105, 2018.
- [19] Charles-Alban Deledalle, Samuel Vaiter, Gabriel Peyré, and Jalal M. Fadili, "Stein Unbiased Gradient estimator of the Risk (SUGAR) for multiple parameter selection," *SIAM Journal on Imaging Sciences*, vol. 7, no. 4, pp. 2448–2487, 2014.
- [20] Sathish Ramani, Thierry Blu, and Michael Unser, "Monte-Carlo SURE: A black-box optimization of regularization parameters for general denoising algorithms," *IEEE Trans. on Image Process.*, vol. 17, no. 9, pp. 1540–1554, 2008.
- [21] Christopher A. Metzler, Arian Maleki, and Richard G. Baraniuk, "From denoising to compressed sensing," *IEEE Transactions on Information Theory*, vol. 62, no. 9, pp. 5117–5144, 2016.
- [22] Hanjie Pan and T. Blu, "An iterative linear expansion of thresholds for  $\ell_1$ -based image restoration," *IEEE Transactions on Image Processing*, vol. 22, no. 9, pp. 3715–3728, 2013.
- [23] K. Dabov, A. Foi, V. Katkovnik, and K. Egiazarian, "Image restoration by sparse 3-D transform-domain collaborative filtering," in *Proc. SPIE Electronic Imaging*, vol. 6812, San Jose, California, USA, Jan. 2008.
- [24] A. Danielyan, V. Katkovnik, and K. Egiazarian, "BM3D frames and variational image deblurring," *IEEE Trans. Image Process.*, vol. 21, no. 4, pp. 1715–1728, 2012.
- [25] Vardan Papyan and Michael Elad, "Multi-scale patch-based image restoration," *IEEE Trans. Image Process.*, vol. 25, no. 1, pp. 249–261, 2016.
- [26] C.J. Schuler, H.C. Burger, S. Harmeling, and B. Scholkopf, "A machine learning approach for non-blind image deconvolution," *Proc. IEEE Int. Conf. Comput. Vision and Pattern Recognition*, pp. 1067–1074, 2013.